

# AUTOMATION AND EVALUATION OF THE UNCERTAINTY IN THE COORDINATE-GRID METHOD

Galina TODOROVA, Valentin DIKOV  
Technical University of Sofia, Bulgaria

**Abstract:** A developed methodology for automated implementation of an experiment using the coordinate-grid method is applied. The presented experimental displacements obtained by means of a specialty designed program system are compared with those obtained by FEM analyses. The uncertainty of the displacements is evaluated too.

**Keywords:** automation of the coordinate-grid method, experimental determination of displacements, displacement uncertainty

## 1. Introduction

The methods for registration of displacements and deformations by means of grids are created in the middle of 20<sup>th</sup> century [1]. These methods allow the temporal distribution of the displacement and deformation fields to be studied when external load is applied. Rulers and micro-scopes have been used for their measurements at initial.

The contemporary digital technique reveals new and much better opportunities for experimental development in many scientific fields including coordinate grid methods. The new approach consists in making of a grid with preliminary chosen geometry on the surface of the studied sample [1, 2]. The image of the so-fixed grid is registered at first before load of the specimen and many times (in equal intervals) during the deformational process. The changes which occur on the specimen surface (independently the specificity of the deformational conditions – plane stress state or plane strain state) cause corresponding grid geometry changes. The last ones are registered in discrete regime by means of a digital microscope and an appropriate computerized system. The digital processing of selected images of deformed grids permits the qualitative and quantitative evaluation of the displacement and/or deformation fields of the observed area. The results thus received could be presented in discrete or interpolated form.

Considering the problems above the improvement of the coordinate-grid method could be realized by its automation in relation to calculation of displacements and their corresponding uncertainty which is the main purpose of this work.

## 2. Principle of the method

A common photo-resist technology is applied on flat specimens as to produce the needed grid [1]. The most appropriate grid's dot patterns have

rectangular [2] or hexagonal [3] disposition. The shape of dot is mostly very small circle or dash.

For the purpose of our experimental study a hexagonal grid with circle dots is used (figure 1).

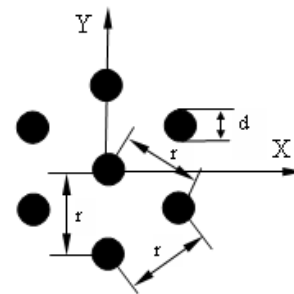


Figure 1. Non-deformed hexagonal element of the grid

Its two important parameters are: the distance ( $r$ ) between two neighbouring dot's gravity centres (DGCs) and the dot's diameter ( $d$ ). In our case  $r \approx 1$  mm and  $d \approx 0.25$  mm.

## 3. Procedure

The automation of the coordinate-grid method is accomplished by the following algorithm:

- /1/ taking pictures (Bitmap-format at equal time intervals) of the grid during its deformation;
- /2/ software processing of the digital images in order to calculate the DGCs positions as well as to evaluate the discrete values of the displacement.

The specialty designed program system realizes next subsequent stages:

- Transformation of the images from coloured to their gray-scale state;
- Image filtering in order to improve the contrast between dot objects and background [4, 5];
- Segmentation of the filtered images in order to separate dot objects from background. The binary images thus obtained include the grid objects;

- Elimination of the objects which outlines cross the boundary of the examined region;
- Evaluation of the DGCs coordinates of the binary image objects towards the coordinate system of the entire image – O\*X\*Y\* (figure 2);
- Determination of the corresponding objects which belong to two consecutive images or between the first image and any other one taken later;
- Transformation of the DGCs coordinates from the image pixels' coordinate O\*X\*Y\* system to the coordinate system OXY (figure 2) where the new origin (O) is the centre of the chosen pixel. This one determines the stress concentrator's apex position in its non-deformed state.
- The mathematical relations by which the OX\*Y\* coordinate system transforms into OXY one are:

$$X = X^* - X_{transform.} + 0.5 \quad [\text{pixels}]$$

$$Y = Y_{transform.} + 0.5 - Y^* \quad [\text{pixels}]$$

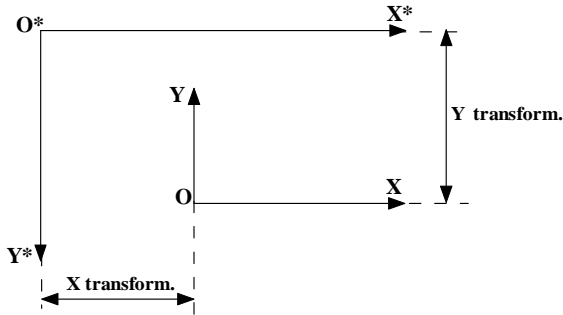


Figure 2. Transformation of the coordinate system O\*X\*Y\* into OXY by  $X_{transform.}$  and  $Y_{transform.}$

### 3.1. Calculation of the displacements

The calculation principle of the displacements of corresponding objects towards X and Y-axis by the coordinates of their DGCs is elucidated on figure 3 [6].

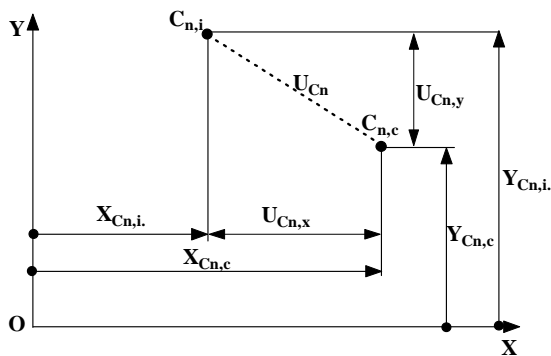


Figure 3. Definition of the displacement

The displacement ( $U_{n,x}$ ) of the  $n^{th}$  object which DGC is moved towards X-axis could be presented as follows:

$$U_{Cn,x} = X_{Cn,c} - X_{Cn,i}$$

The displacement towards Y-axis could be analogically presented by the equation:

$$U_{Cn,y} = Y_{Cn,c} - Y_{Cn,i}$$

where:

- $X_{Cn,c}$  is the Current coordinate of the  $n^{th}$  DGC towards X-axis;
- $X_{Cn,i}$  – the Initial coordinate of the same ( $n^{th}$ ) DGC towards X-axis;
- $Y_{Cn,c}$  – the Current coordinate of the  $n^{th}$  DGC towards Y-axis;
- $Y_{Cn,i}$  – the Initial coordinate of the same ( $n^{th}$ ) DGC towards Y-axis.

### 3.2. Evaluation of the uncertainty for the displacements

The computed dot's positions (of the experimental grid) differ from the exact ones. For evaluation the computational uncertainty for the discrete displacement values an approach based on the assumption that these differences could be presented by the sum of random and systematic errors is used. Hence, the value of the  $f_n$  function which depends on the position of the  $n^{th}$  point is also depending on an analogous sum. Such computational uncertainty is assumed to be equal to the linear member from a Taylor series of the decomposed displacement function [7]. This linear member /equation (1)/ determines the increase of the function ( $\Delta f_n$ ) at the  $n^{th}$  point which coordinates are  $(x_n + \Delta x, y_n + \Delta y)$  [8]:

$$f_n(x_n + \Delta x, y_n + \Delta y) = f(x_n, y_n) + \frac{1}{1!} \left( \frac{\partial}{\partial x} \Delta x + \frac{\partial}{\partial y} \Delta y \right) f(x_n, y_n) + \frac{1}{2!} \left( \frac{\partial}{\partial x} \Delta x + \frac{\partial}{\partial y} \Delta y \right)^2 f(x_n, y_n) + \dots + R_n^*$$

where  $R_n^*$  is the remaining member of the Taylor's series.

For the calculation of the linear member of the Taylor's series it is necessary to find the largest linear deviation for DGCs along the X-axis –  $\delta_x$  and analogous for Y-axis –  $\delta_y$  from the initial image which corresponds to non-deformed state. They are equalized to the increases in the Taylor's series –  $\Delta x$  and  $\Delta y$ .

The algorithm for the computational uncertainty when  $\Delta x > 0$  and  $\Delta y > 0$  is illustrated on Figure 4. The function  $f_n$  which is depending on DGCs coordinates represents the displacement  $U_y$  (along the Y-axis).

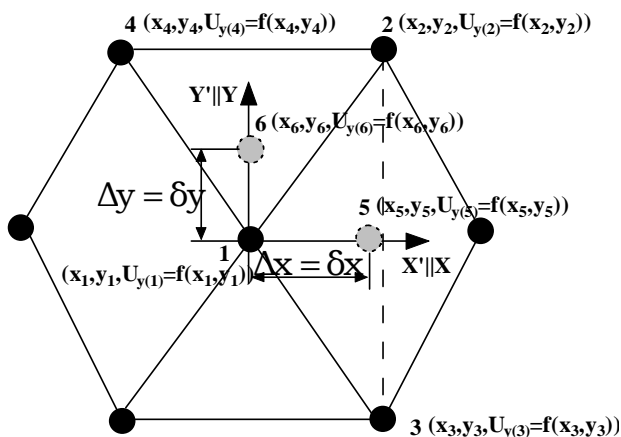


Figure 4. Grid-element representing the idea of the uncertainty for the displacement

Concerning the uncertainty of the displacement  $U_{y(1)}$  at point 1 i.e.  $n = 1$  (figure 4) it could be represented by:

- The coordinates of point 5 by the equations:

$$x_5 = x_1 + \delta_x$$

$$y_5 = y_1$$

- The coordinates of point 6 by the equations:

$$x_6 = x_1$$

$$y_6 = y_1 + \delta_y$$

So for the displacement  $U_{y_5}$  towards X-axis (figure 4, point 5, considering the triangle defined by points  $(x_1, y_1)$ ,  $(x_2, y_2)$  and  $(x_3, y_3)$ ) the calculation is presented by the linearization:

$$U_{y(5)} = a_1 U_{y(1)} + a_2 U_{y(2)} + a_3 U_{y(3)}$$

where  $a_1$ ,  $a_2$  and  $a_3$  are weight coefficients, defined from the system of linear equations:

$$\begin{cases} a_1 x_1 + a_2 x_2 + a_3 x_3 = x_5 \\ a_1 y_1 + a_2 y_2 + a_3 y_3 = y_5 \\ a_1 + a_2 + a_3 = 1 \end{cases}$$

Thus the increment towards X-axis ( $\Delta U_{y_{x(1)}}$ ) of the considered function calculates from:

$$\Delta U_{y_{x(1)}} = U_{y(5)} - U_{y(1)}$$

An analogical approach for the displacement towards Y-axis of  $y_6$  (respectively  $z_6$ ) is applied, but the triangle now is defined by points  $(x_1, y_1)$ ,  $(x_2, y_2)$  and  $(x_4, y_4)$ . Following the procedure shown above the increment towards Y-axis is:

$$\Delta U_{y_{y(1)}} = U_{y(6)} - U_{y(1)}$$

Finally, the common increment which evaluates the uncertainty for the considered discrete value –  $U_{y(1)}$  is:

$$\Delta U_{y(1)} = \Delta U_{y_{x(1)}} + \Delta U_{y_{y(1)}}$$

### 3.3. Scale of the displacements

In this study the experimental hexagonal grid parameter “ $r$ ” is 1 mm. The procedure of scale

recalculations is based on the assumption that it is possible to calculate the number of the pixels which correspond to the mean non-deformed circle radiuses which are in the whole observed area. The developed software is written in Delphi.

## 4. Experiment

The plate shaped specimens are made of low carbon steel sheet which thickness is 1.5 mm. In their middle part a  $16 \times 0.1$  mm slot is made which orientation towards the direction of the external load is at an angle of  $90^\circ$ . The specimen geometry and the analysed region (dotted area) are shown on figure 5.

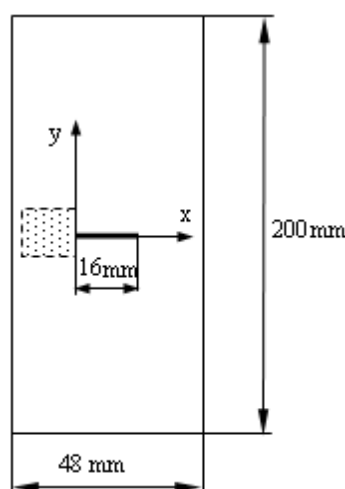


Figure 5. Specimen's geometry, stress concentrator and analysed region (dotted area) in front of it

An electro-mechanical testing machine type Instron-1185 is used. The specimen's deformation is accomplished at a speed of 0.5mm/min. During the experimental load the grid deformation in the region around the one of the slot ends is studied (figure 5). The grid geometry changes are registered by means of a digital microscope – Dino Light Pro (CMOS resolution 1280x1024) – at every 30 seconds. The microscope is connected to a PC (figure 6) where simultaneous registration of the corresponding force is kept too. It is important to note that the microscope is immovably fixed to the testing machine body. So the microscope's range of vision ensures an initial coordinate system towards which the real DGC displacements could be calculated.

## 5. Results and Discussion

A force-extension curve of a specimen with a  $90^\circ$  positioned stress concentrator is presented on the figure 7. The points on the curve correspond to the current time at which a digital picture was taken.



Figure 6. Experimental set for simultaneous registration of image-deformation changes

On the figure 8 are shown the values of the discrete DGCs' displacements when the specimen is under the load of 5880 N (point 3 on the figure 7).

As a rule – only the values of the displacement field which remain in the microscope's range of vision during the deformation are taken into account. Subsequently, only these dots which are positioned in front of the forming crack are in the focus of our interest. The data on the labels belonging to every DGC must be read as follows: upside – the particular displacement; downside – its uncertainty.

From a practical point of view it is interesting to compare the results for the displacement distribution obtained by proposed automated coordinate-grid method with these ones derived from the FEM analyses.

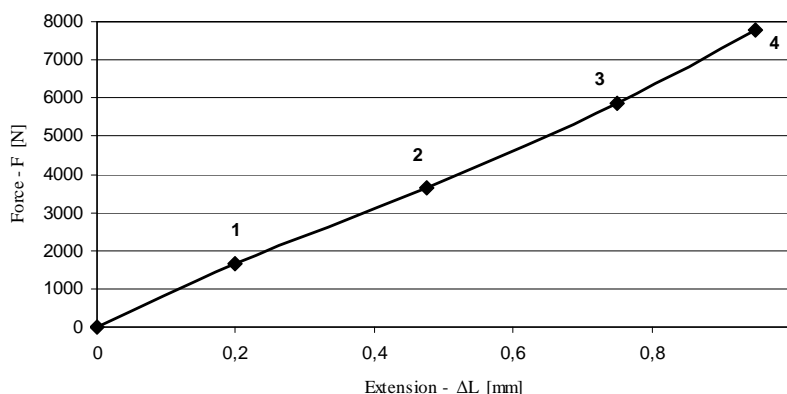


Figure 7. Force-extension curve of the specimen with a stress concentrator positioned at 90° towards the load direction

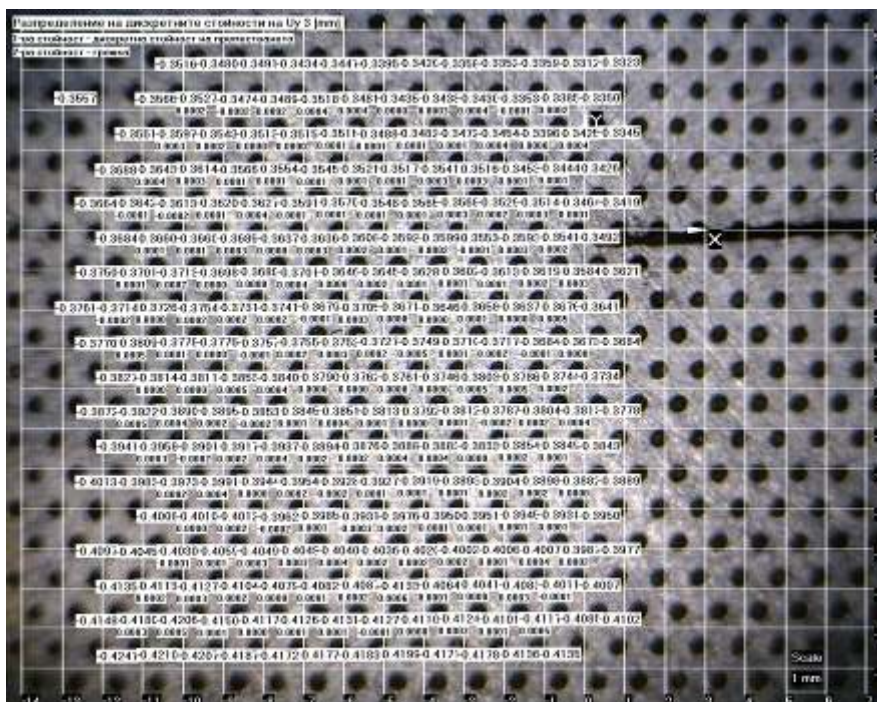


Figure 8. A grid image of a specimen with a 90° positioned slot under a load of 5880 [N] The values (in mm) of the discrete DGCs' displacements and their corresponding uncertainties are shown

ANSYS is especially suitable for comparative mechanical investigations between experimentally and numerically (FEM) evaluated results. The ANSYS model uses isoparametric eight-node finite elements – plane 183 (figure 9-a) which predefined edge length is 0.5 mm. The artificial material model used here is linear-isotropic which modulus of elasticity is 206 GPa and Poisson’s ratio is 0.28. The numerical results refer to experimentally investigated area only. The finite element mesh in this region is shown on figure 9-b.

The comparison between the two approaches –

the automated coordinate-grid method and FEM could be accomplished on the graphs presented on figure 10 and 11. All displacements are presented by isolines (joining the points that have the same values) for the set of experimental conditions. The beginning of the coordinate system (figure 5) is in the left end of the slot – at the so-called stress concentrator. The data thus received refer to the Y-direction during the specimen treating at a load of 1646.4 N and 5880 N respectively. The dimensions of the analyzed rectangular area are 13×14 mm.

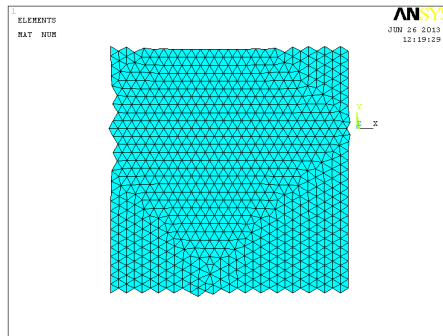
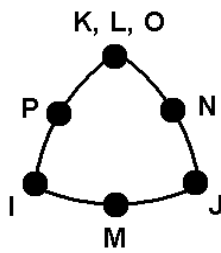


Figure 9. (a) Isoparametric finite element – plane 183; (b) A finite element mesh of the examined region

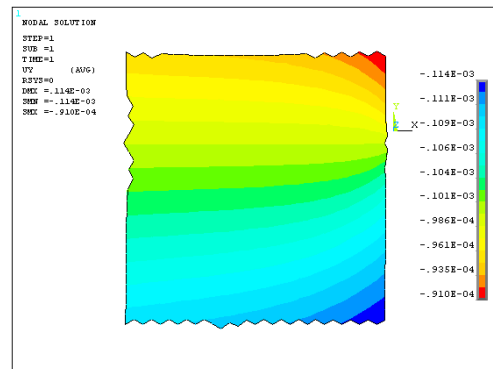
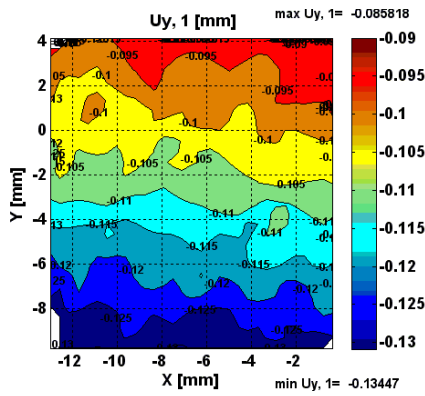


Figure 10. Interpolated (a) experimentally -  $U_{y1}$  [mm] and (b) numerically FEM (ANSYS) -  $U_{y1}$  [mm] obtained data for the displacement distributions towards Y-axis at a load of 1646.4 [N]

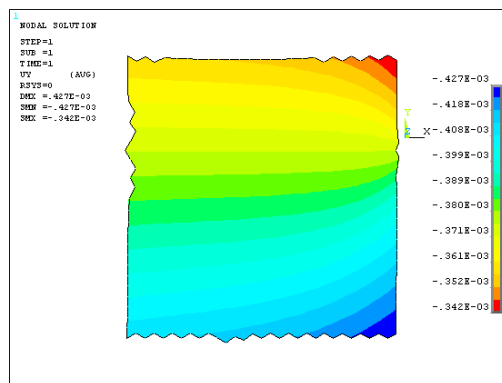
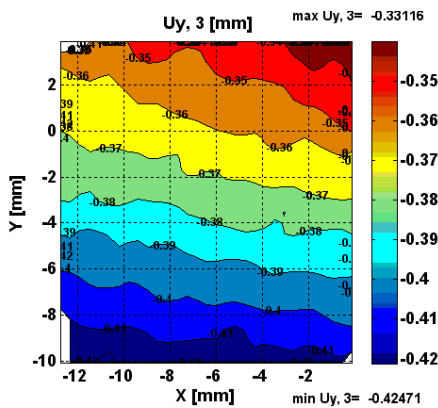


Figure 11. Interpolated (a) experimentally -  $U_{y3}$  [mm] and (b) numerically FEM (ANSYS) -  $U_{y3}$  [mm] obtained data for the displacement distributions towards Y-axis at a load of 5880 [N]

The comparison between experimental and numerical displacement distributions ( $U_y$ ) reveals that the experimental and numerical results towards Y-axis are similar in the shape of their isolines and values as well.

An initially surprising experimental result was the irregularities of the isolines. In our opinion the lack of gradual changes in displacement distributions is due to the structural non homogeneity of the real specimen's material. It is a result of inherent differences between shapes and sizes of the forming crystals.

$$\Delta U_{y3,\min} = \frac{U_{y3,FEM} - \min U_{y3,EXP}}{U_{y3,FEM}} = \frac{-0.375 - (-0.3685)}{-0.375} \cdot 100 = 1.73\%$$

$$\Delta U_{y3,\max} = \frac{U_{y3,FEM} - \max U_{y3,EXP}}{U_{y3,FEM}} = \frac{-0.375 - (-0.3492)}{-0.375} \cdot 100 = 6.88\%$$

The calculated relative differences are in good agreement with the necessary accuracy for such investigations. If the grid is finer it can be expected that the relative differences between experimental and numerical results will become smaller.

## 7. Conclusions

A developed methodology for automated implementation of an experiment using the coordinate-grid method is applied.

The coordinate grid method is successfully automated by means of a speciality developed program system for image processing and post processing calculations.

The developed program system allows calculation of the discrete values of the displacement fields and additionally calculates corresponding uncertainties of the calculated values of the displacements.

The presented experimental results are compared with those obtained by FEM analyses. The corresponding relative differences between numerical and experimental values for displacements are in good agreement with the necessary accuracy for such investigations.

The experimental results show that the usage of a CMOS sensor which resolution is at least 1280×1024 pixels combined with an optical magnitude of 30X are sufficient for solving practical problems of a such kind.

This experimental method allows easy calculation of distances from some defect such as crack tip and DGCs in the same investigated area.

The process of deformation begins initially in the weaker volumes of the material which are statistically dispersed. Therefore it is impossible to achieve uniform displacements of the material points at their initial stages of deformation.

An additional opportunity is the possibility to compare the corresponding relative differences between numerical and experimental data.

For example, the calculations below are accomplished for minimal and maximal values for  $U_{y(3)}$  displacements. Towards the horizontal line in front of the stress concentrator they are computed as follows:

In this meaning, the coordinate grid method is suitable for experimental investigation in the area of fracture mechanics for plane problems when stress functions are used.

## References

1. Parks, V.J. (1969) *The grid method*. Experimental Mechanics, ISSN 0014-4851, Vol. 9, no. 7, p. 27N-33N
2. Matvienko, U.G. (2006) *Modeli i kriterii mehaniki razrushenia (Models and criteria of fracture mechanics)*. Fizmatlit, ISBN 2-9221-0669-4, Russia, p. 197 (in Russian)
3. Vavrik, D., Zemankova, J. (2004) *Crack instability in ductile materials analyzed by the method of interpolated ellipses*. Experimental Mechanics, ISSN 0014-4851, Vol. 44, no. 4, (August 2004), p. 327-335
4. Lazarova, M., Angelova, M. (2007) *Rakovodstvo za laboratorni uprazhnenia po komputarno zrenie i razpoznavane na obrazi (Laboratory experiments on Computer Vision and Pattern Recognition)*. Technical University-Sofia, ISBN 978-954-438-675-7, Sofia, Bulgaria, p. 12 (in Bulgarian)
5. Bovik, A. (2009) *The essential guide to image processing*. Elsevier, ISBN: 978-0-12-374457-9, p. 42
6. Varbanov, H., Tepavicharov, A., Ganeev, T. (1992) *Prilozhna teoria na elastichnostta i plastichnostta (Applied Theory of Elasticity and Plasticity)*. Technika, ISBN 954-03-0043-6, Sofia, Bulgaria, p. 23 (in Bulgarian)
7. Del, G.D., Novikov, N.A. (1979) *Metod delitelnih setok (The method of dividing nets)*. Mashinostroene, Moscow, USSR, p. 8 (in Russian)
8. Dimova-Nacheva, V., et al. (1975) *Metodichesko rakovodstvo za reshavane na zadachi po vissha matematika (Methodological guidance for solving problems in higher mathematics) (part-1)*. Technika, Sofia, Bulgaria, p. 231 (in Bulgarian)

Received in August 2013  
(and revised form in October 2013)